Correlation Effects in Disordered Metallic Photonic Crystal Slabs

D. Nau,[1,2] A. Schönhardt,[1] Ch. Bauer,[3] A. Christ,[3] T. Zentgraf,[3] J. Kuhl,[3] M. W. Klein,[4] and H. Giessen[2,*]

[1]*Institut für Angewandte Physik, Universität Bonn, 53115 Bonn, Germany*
[2]*4. Physikalisches Institut, Universität Stuttgart, 70550 Stuttgart, Germany*
[3]*Max-Planck-Institut für Festkörperforschung, 70569 Stuttgart, Germany*
[4]*Institut für Angewandte Physik, Universität Karlsruhe (TH), 76131 Karlsruhe, Germany*

(Received 2 October 2006; published 30 March 2007)

We analyze the influence of correlations on the optical properties of disordered metallic photonic crystal slabs experimentally and theoretically. Different disorder models with different nearest-neighbor correlations are considered. We present a theory that allows us to quantitatively calculate the optical properties of the different samples. We find that different kinds of correlations produce characteristic spectral features such as peak reduction and inhomogeneous broadening. These features are caused by reduced excitation efficiencies and the excitation of multiple resonances.

DOI: 10.1103/PhysRevLett.98.133902 PACS numbers: 42.70.Qs, 64.60.Cn, 78.20.Bh, 78.40.Pg

Since the early days of photonic crystals, disorder has played a major role. Disorder due to fabrication errors is usually an intrinsic attribute of photonic crystals, which inevitably influences their optical properties [1]. Hence, a detailed understanding of disorder can help to improve photonic band gap materials [2]. Additionally, the potential to localize light in disordered materials [3] has led to stimulating discussions about the influence of correlations on the localization length [4–6]. Most work so far has discussed small disorder amounts, which can be handled analytically by using a perturbative theoretical approach [2]. Other publications have focused on experimental investigations, comparable to finite difference time domain simulations [7]. As a consequence, a detailed analysis of the optical properties of disordered photonic crystals is of interest not only for possible applications but also from a fundamental point of view. In this Letter, we investigate the influence of different nearest-neighbor correlations on the optical properties of disordered metallic photonic crystal slabs (MPCSs) systematically in experiment and theory. We present a concept that allows for the calculation of these optical properties and for direct interpretation of the experimental data. Our model is not restricted to small amounts of disorder as it allows one to intuitively guess the actual shape of the optical properties in strongly disordered photonic crystals.

The considered model system consists of gold nanowires on top of a dielectric waveguide layer [Fig. 1(a)]. It was previously reported that the linear optical properties of a MPCS can be tailored by an appropriate arrangement of the nanostructures [8]. Characteristic spectral features and a pronounced band structure were found [9]. The electronic resonance of the particle plasmons and the optical quasiguided mode in the waveguide can couple strongly to form a waveguide-plasmon polariton. In metal wires, the particle plasmon and, hence, the polariton are excited only for a light polarization perpendicular to the wires (TM polarization). For a light polarization along the wires (TE), only the quasiguided mode can be excited.

We fabricated one-dimensional gold gratings on top of a 140-nm-thick indium tin oxide (ITO) waveguide layer that was deposited on a quartz substrate [Fig. 1(a)]. The width of the wires was 100 nm, and the height was 20 nm. The optical properties of these MPCSs were measured at normal light incidence with a white-light transmission setup with an aperture angle of about 0.2° [9]. As electron-beam lithography was used to fabricate the samples, we were able to control the nanostructures' positions and shapes with very high accuracy. This process provides a powerful tool for the introduction of artificial disorder with a well-defined type and strength. When measuring the extinction [$-\ln(T)$, T: transmission] of these structures, the influence of disorder type and amount on the optical properties of MPCSs can be studied.

We consider two different models of positional disorder: uncorrelated and correlated disorder. In the first model, the positions of neighboring nanowires are uncorrelated; they are varied around their positions in the perfect grid [resembling a "frozen phonon," Fig. 1(b)]. Starting at position x_0, the position of nanowire i is given by

$$x_i = x_0 + id_0 + \Delta x_i, \tag{1}$$

where d_0 is the period of the perfect grating and Δx_i is the

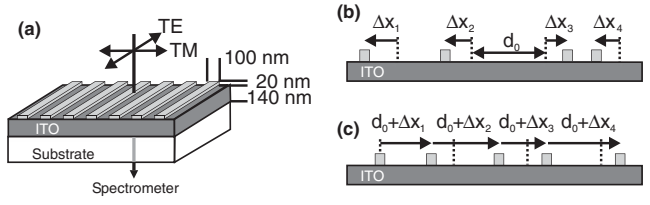

FIG. 1. (a) Metallic photonic crystal slab structure consisting of a gold grating on top of a waveguide layer. The light propagates through the sample at normal incidence. TE and TM indicate the direction of the electric field polarization. (b),(c) Schematic view of uncorrelated and correlated disorder, respectively. Dotted lines indicate the center positions of the perfect grating with period d_0.

variation of the ith position. In the second model, the positions x_i and x_{i-1} of neighbors are correlated [Fig. 1(c)], which resembles long-range disorder. Therefore, x_i includes all variations of the preceding nanowires:

$$x_i = x_{i-1} + d_0 + \Delta x_i = x_0 + id_0 + \sum_{n=1}^{i} \Delta x_n. \quad (2)$$

The variations Δx follow a normal distribution with a full width at half maximum w. Giving w as a fraction of d_0 quantifies the disorder amount $a[\%] = w/d_0 \times 100$.

The simulation of the optical properties of the samples is done in several steps. First, the spatial arrangement of all nanowires in a fabricated sample is considered, and the Fourier transform of this arrangement is calculated. Figure 2 shows results for exemplary arrangements with uncorrelated and correlated disorder around the first reciprocal lattice vector $g_0 = 2\pi/d_0$ ($d_0 = 400$ nm). Pronounced differences in the distribution of the Fourier amplitudes $|A|$ at different momenta k are observable. In the case of no disorder, a sharp δ-shaped peak appears at $k = g_0$. Increasing uncorrelated disorder reduces the amplitude of this Fourier component. Correlated disorder also diminishes the amplitude of this peak but for smaller amounts of disorder. The peak vanishes for an amount of about 50%, in comparison with an amount of 80% in the uncorrelated model. Furthermore, additional peaks arise at $k \neq g_0$, causing an inhomogeneous broadening in the Fourier spectrum. These differences are the key to understanding the spectral characteristics of the various disorder models.

To enlighten the differences of the disorder models, we make use of the similarity of the Fourier analysis with the results obtained in x-ray diffraction experiments [10]. There, the effect of reduced amplitudes is described by the Debye-Waller factor for thermal movement of the atoms. The Fourier transform of correlated disorder resembles the diffraction pattern of amorphous solids or liquids, i.e., systems with no long-range ordering but nearest-neighbor correlations [11,12]. The frozen phonon disorder rather resembles scattering in hot solids.

In a next step, we consider the dispersion relation of the MPCS. The TE and TM quasiguided modes depend on the lateral wave vector, and they are given by the solutions of transcendental equations [13]. In TM polarization, the quasiguided mode at energy $E_{\mathrm{wg}}(k_j)$ couples to the plasmon at constant energy E_{pl}. This results in a typical polariton dispersion with two dispersion branches in ordered MPCSs [9,14]. For normal light incidence, the period or, more generally, the Fourier spectrum determines the energies of the excited resonances [15]. Their amplitudes are given by the amplitudes of the Fourier components and, hence, the lattice structure [16]. Combining Fourier analysis and dispersion of the sample yields a transformation of the Fourier peaks from k space into energy space: Each Fourier component at k_j excites resonances with energies $E_j = E(k_j)$ and amplitudes $I_j \propto |A_j|^2$.

To finally calculate the optical spectra of the samples, we plug the energies E_j and amplitudes $|A_j|$ of the excited resonances into suitably chosen line shape functions. In TE polarization, the extinction $\alpha_j^{\mathrm{TE}}(E)$ is characterized by a Fano-type line shape [9,17]. In TM polarization, the absorption of the system can be modeled with two coupled Lorentzian oscillators [18]. For simplicity, we identify the extinction with this absorption [18]:

$$\alpha^{\mathrm{TM}}(E) = \alpha_N \frac{4\gamma_{\mathrm{pl}}^2 E^2 [E^2 - E_{\mathrm{wg}}^2 - (q_{\mathrm{wg}}/q_{\mathrm{pl}})E_c^2]^2}{1/\hbar^2[(E^2 - E_{\mathrm{pl}}^2)(E^2 - E_{\mathrm{wg}}^2) - E_c^4]^2 + 4\gamma_{\mathrm{pl}}^2 E^2 (E^2 - E_{\mathrm{wg}}^2)^2}, \quad (3)$$

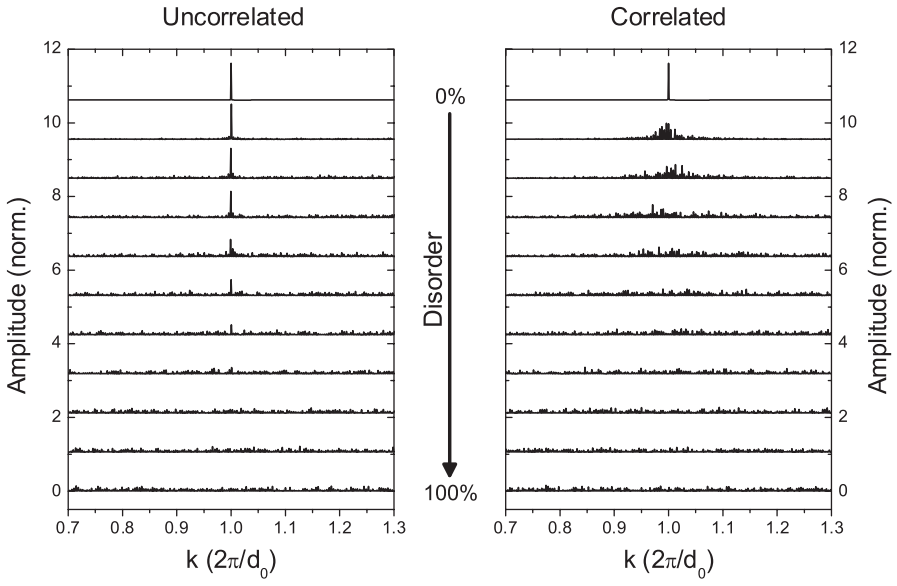

FIG. 2. Fourier analysis of exemplary structures with uncorrelated and correlated disorder. The disorder was increased in steps of 10%. Each structure consisted of 1000 nanowires with $d_0 = 400$ nm. The curves are shifted for clarity.

with α_N as a scaling factor depending on the density of the excited pairs of plasmon and quasiguided mode, and E_l, γ_l, and q_l ($l = \mathrm{pl}, \mathrm{wg}$) as resonance energies, homogeneous half-widths, and oscillator strengths of the uncoupled system. The waveguide-plasmon coupling strength is denoted as E_c^2. Thus, each Fourier component at k_j yields an extinction $\alpha_j^{\mathrm{pol}}(E)$, where "pol" denotes the polarization (TE or TM). The total extinction $\alpha^{\mathrm{pol}}(E)$ of the disordered samples is the sum over all $\alpha_j^{\mathrm{pol}}(E)$:

$$\alpha^{\mathrm{pol}}(E) = \sum_j \alpha_j^{\mathrm{pol}}(E). \tag{4}$$

The necessary TE and TM parameters are determined by fitting the individual line shape functions to the measured extinction spectra of the perfect samples. They are then used as disorder-independent parameters in the calculation of $\alpha_j^{\mathrm{pol}}(E)$ and $\alpha^{\mathrm{pol}}(E)$. Adapting the polariton picture to Eq. (3) means that each Fourier component excites simultaneously a plasmon and a quasiguided mode as a pair of coupled resonances in TM polarization. Hence, I_j affects directly the density-dependent factor α_N of these pairs in Eq. (3). We set $\alpha_N/\alpha_0 = I_j = |A_j|^2$, where α_0 is the maximum extinction as determined from the fits of the perfect samples. An illustration of the model is presented in Fig. 3 with spatial Fourier analysis, TE and TM dispersion, and the resulting extinction spectra in energy space.

Figure 4 shows measured extinction spectra for uncorrelated and correlated disorder. They are compared with the simulations that help to completely understand the observations. We notice good agreement of measurements and simulations. In TE polarization (upper half of Fig. 4), the typical Fano-like resonance of the quasiguided mode can be observed for no disorder. Increasing uncorrelated disorder causes a reduction of its amplitude and a vanishing at about 70% disorder. The resonance width is not affected. Correlated disorder reduces the resonance amplitude more drastically, which results in a complete vanishing at 50% disorder. Additionally, a strong broadening of the resonance peak can be observed. All of these findings can be immediately understood, since for TE polarization the extinction is simply a convolution of the spatial Fourier spectrum (see Fig. 2 as an example) with the Fano line shape. For correlated disorder, the nanowires' arrangement acts as a superposition of gratings with different periods. As a result, multiple quasiguided modes are excited in a wide energy range [19], causing a broadening of the extinction peak. The peak reduction for uncorrelated disorder goes along with a slight peak shift to lower energies. The latter is caused by the disorder influence on the TE band structure [20], which was not included in the simulations.

The lower half of Fig. 4 shows results for TM polarization. For no disorder (uppermost curves), two extinction maxima, corresponding to the lower and upper polariton branches, appear. With increasing disorder, the measured extinction curves show a distinctively different behavior for uncorrelated and correlated disorder. In the first case,

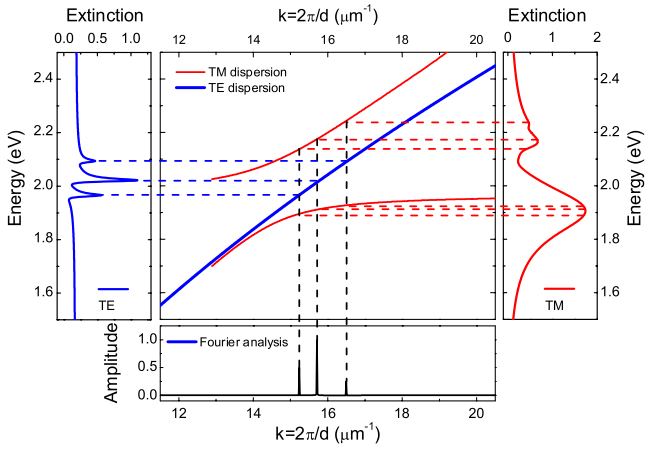

FIG. 3 (color online). Transformation of exemplary Fourier peaks from k space into energy space via the dispersion relations. Schematic line shape functions are added in energy space to yield $\alpha^{\mathrm{TE}}(E)$ and $\alpha^{\mathrm{TM}}(E)$.

the upper polariton branch vanishes, resulting in a broadened particle plasmon peak for maximum disorder. We also note a decreased energy separation between the branches for increased disorder. In the second case, both polariton branches show a broadening with increased disorder; for maximum disorder, again a single broad particle plasmon peak arises. As for TE polarization, the spatial Fourier analysis helps to explain these effects. For uncorrelated disorder, the decreasing Fourier peak amplitude indicates a decrease of the weighted polariton double-peak contribution to the spectrum. Simultaneously, the increasing background in the Fourier spectrum increases the contribution of plasmons coupled to waveguides of arbitrary E_{wg}, appearing as the simple plasmon at E_{pl}. For correlated disorder, the broadening of both polariton branches originates from the excitation of multiple resonances at energies varying in a certain, finite spectral range.

The measurements in TM polarization are also well explained by our theoretical model; however, some smaller details are not as well reproduced as in TE polarization. This is probably due to the omission of near-field coupling of the individual nanowires [21] in the disorder arrangement, which presumably causes the strong broadening of the pure plasmon resonance at large disorder. We account this effect to be responsible also for the pronounced maxima and minima at moderate correlated disorder. Note that a small contribution to the resonance broadening originates from variations of the nanowires' width on the order of a few nanometers due to fabrication imperfections. The decreased branch separation for increased uncorrelated disorder, which manifests itself in the smaller splitting between the polariton branches, can be explained by the dependence of the waveguide-plasmon coupling strength E_c^2 on defects and disorder in MPCSs [15,20]. A more detailed theory, addressing these effects and the dispersion in disordered MPCSs, will be presented in future work.

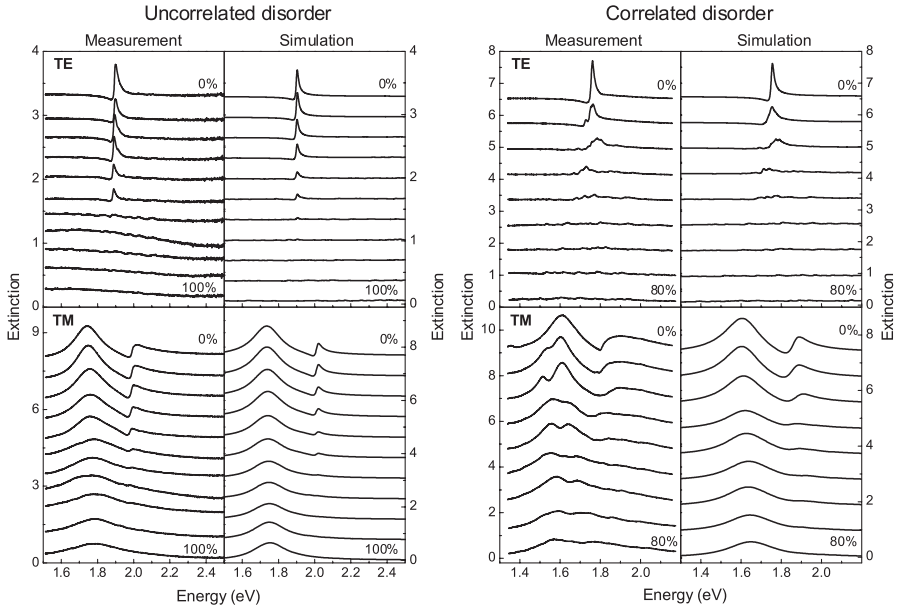

FIG. 4. Measured and simulated extinction spectra for different disordered samples in TE and TM polarization. Left panel: Results for uncorrelated disorder, $d_0 = 430$ nm. Right panel: Results for correlated disorder, $d_0 = 475$ nm. The disorder was increased in steps of 10%. The individual spectra are shifted for clarity.

To summarize, we have presented a detailed analysis of the influence of nearest-neighbor correlations on the optical properties of disordered metallic photonic crystal slabs. Our theory allows for the modeling of optical properties in different disorder types. Combining the Fourier analysis of the spatial grating arrangement with the dispersion of the structure predicts the energies and amplitudes of the excited resonances. Theoretical and experimental results show good agreement. It was shown that uncorrelated disorder reduces the amplitudes of spectral peaks. Correlated disorder results in additional broadening of the spectral features, which is caused by the excitation of multiple resonances. Our results may help to estimate the consequences of imperfections in the fabrication of MPCS-based devices in the limit of large disorder. Future tasks include light localization and investigating the polariton coupling and dispersion relations in disordered MPCSs in more detail.

We thank H. Kroha and S. G. Tikhodeev for fruitful discussions and the teams of R. Langen and K. D. Krause for technical support. We thank P. Thomas (Marburg) and S. Dietrich (Stuttgart) for their contributions to this work. Financial support by the German BMBF (FKZ 13N8340/1) and DFG (FOR 557 and SPP 1113) is gratefully acknowledged.

*Electronic address: giessen@physik.uni-stuttgart.de

[1] A. F. Koenderink, A. Lagendijk, and W. L. Vos, Phys. Rev. B **72**, 153102 (2005).
[2] S. Hughes, L. Ramunno, J. F. Young, and J. E. Sipe, Phys. Rev. Lett. **94**, 033903 (2005).
[3] S. John, Phys. Rev. Lett. **58**, 2486 (1987).
[4] D. H. Dunlap *et al.*, Phys. Rev. Lett. **65**, 88 (1990).
[5] C. M. Soukoulis, M. J. Velgakis, and E. N. Economou, Phys. Rev. B **50**, 5110 (1994).
[6] F. M. Izrailev and A. A. Krokhin, Phys. Rev. Lett. **82**, 4062 (1999).
[7] M. Bayindir *et al.*, Phys. Rev. B **64**, 195113 (2001).
[8] S. Linden, J. Kuhl, and H. Giessen, Phys. Rev. Lett. **86**, 4688 (2001).
[9] A. Christ, S. G. Tikhodeev, N. A. Gippius, J. Kuhl, and H. Giessen, Phys. Rev. Lett. **91**, 183901 (2003).
[10] C. Kittel, *Introduction to Solid State Physics* (Wiley, New York, 1996).
[11] J. M. Ziman, *Models of Disorder* (Cambridge University Press, Cambridge, England, 1979).
[12] L. F. Rojas-Ochoa *et al.*, Phys. Rev. Lett. **93**, 073903 (2004).
[13] M. K. Barnoski, *Introduction to Integrated Optics* (Plenum, New York, 1974).
[14] A. Christ *et al.*, Phys. Rev. B **70**, 125113 (2004).
[15] T. Zentgraf *et al.*, Phys. Rev. B **73**, 115103 (2006).
[16] A. Yariv and M. Nakamura, IEEE J. Quantum Electron. **13**, 233 (1977).
[17] S. Fan and J. D. Joannopoulos, Phys. Rev. B **65**, 235112 (2002).
[18] M. W. Klein, T. Tritschler, M. Wegener, and S. Linden, Phys. Rev. B **72**, 115113 (2005).
[19] D. Marcuse, Bell Syst. Tech. J. **48**, 3187 (1969).
[20] D. Nau *et al.*, Phys. Status Solidi B **244**, 1262 (2007).
[21] W. Rechberger *et al.*, Opt. Commun. **220**, 137 (2003).